THE EFFECTS OF CAVITY GEOMETRY ON AN ASPIRATED COMPRESSOR CASCADE

SHUANG GUO

State Key Laboratory of Structural Analysis for Industrial Equipment, School of Aeronautics and Astronautics,
Dalian University of Technology, Dalian, China; e-mail: sguo@dlut.edu.cn

HUA-WEI LU

Marine Engineering College, Dalian Maritime University, Dalian, China

JIE LIU

AVIC Shenyang Engine Design and Resesrch Institute, Shenyang, China

CHUI-JIE WU

State Key Laboratory of Structural Analysis for Industrial Equipment, School of Aeronautics and Astronautics,
Dalian University of Technology, Dalian, China

The impact of the bleed off-take cavity within aspirated blades on the aerodynamic performance of a highly loaded compressor cascade was explored. Three-dimensional Navier-Stokes simulations were conducted in rectangular compressor cascades after validation against experimental results were done. Five different off-take configurations with varying suction location were numerically evaluated. The results show that the regularities of the suction flow distribution on the suction slot inlet greatly influence the benefits of boundary layer suction. The distribution style greatly depends not only on the flow condition of the blade passage, but also on the realization of the suction process and the geometry of the cavity inside the aspirated blade. The low kinetic fluid in the endwall region compared with that around the midspan is usually prone to be sucked into the suction slot. The distribution of the suction mass flow along the spanwise direction would be symmetrical if the suction position is properly selected and the inside off-take cavity is well designed, even though the bleeding system has been simplified to be asymmetrical as employed in the present document.

Key word: highly loaded compressor cascade, boundary layer suction, suction flow distribution, off-take cavity

Nomenclature

b, B	–	blade chord and axial blade chord, respectively, [m]
DF	–	diffusion factor
h, t	–	blade height and blade pitch, respectively, [m]
i	–	incidence, [deg]
P	–	pressure, [Pa]
Re	–	Reynolds number, [–]
U	–	inlet velocity, [m/s]
w	–	width of suction slot
α_{1p}, α_{2p}	–	inlet and outlet metal angle, respectively, [deg]
β	–	overall suction flow rate relative to inlet mass flow, [–]
β_t	–	stagger angle, [deg]
θ	–	blade camber, [deg]
σ	–	chord to pitch ratio, solidity, [–]
ω	–	total pressure coefficient, [–]

and ORI – baseline scheme without suction slot; SS1, SS2, SS3, SS4, SS5 – schemes with suction slot at 25%, 35%, 48%, 60% and 70% blade chord, respectively.

Subscripts: 0 – stagnation, 1 – inlet, 2 – outlet, t – total, v – velocity, m – overall mass-averaged, exp – experiment, cal – calculation.

Superscripts: $\overline{(\cdot)}$ – relative value.

1. Introduction

The development of aircraft engines demands for higher aerodynamic loading of each individual compressor stage. Therefore, the highly loaded compressor cascade is widely investigated in the purpose of further enhancing the pressure rising capacity of the compression system, and furthermore, achieving a higher thrust-weight ratio. The boundary layer suction technology (BLS) is applied into the aircraft engine to extract a high entropy fluid out from the compressor cascades through the blade surfaces or the endwalls. The benefits of BLS on the aerodynamic performance were already predicated in 1971 (Loughery and Horn, 1971). BLS is also proved to have a great potential to break traditional barriers of the aerodynamic blade loading by increasing the flow turning (Wennerstrom, 1990).

The comprehensive works of MIT (e.g. Kerrebrock *et al.*, 1997, 1998; Reijnen, 1997; Schuler *et al.*, 2000; Merchant et al 2000, 2004) demonstrated that the BLS technology as one of the most effective active flow controls could aid to achieve pronounced improvement in terms of suppressing the flow separation, enhancing the aerodynamic loading capability and reducing the cascade losses.

The aspirated cascades could be used to replace tandem cascades since the blade loading is enlarged. Both the weight and the length of the engine would be effectively reduced (Zhao *et al.*, 2010). In the transonic compressor cascades, the BLS technology is also applied to postpone the oblique shock occurring at the blade leading edge so as to avoid the interaction between the multiple shock waves and the boundary layer on the adjacent blade (Wang *et al.*, 2012).

A major challenge for the BLS technology into application is mainly about the optimal suction position and the suction flow rate. Song *et al.* (2005) and Chen *et al.* (2005, 2006) carried out an extensive numerical investigation in order to figure out the optimal suction parameters in a highly loaded compressor cascade under different solidities and working conditions. Their works suggested that the optimal suction location might be found just in the vicinity of the separation point of the corner region, so the decision about the suction stratagem should be made according to the practical flow field conditions.

The computational domain in most reported numerical investigations on BLS was just a single main flow passage or, at most, one flow passage associated with the suction slot region since the improvement of the blade passage flow field is generally focused on. A small portion of the suction surface or the outlet of the suction slot was numerically defined as an outlet with a certain amount of permanent mass flow or a fixed static pressure. The setting may lead to different regularities of the suction flow distribution as well as different conclusions on the optimal suction position and suction flow rate compared with that of the real condition.

Gmelin *et al.* (2011) succeeded in diminishing the corner separation by steady boundary layer removal from the corner region. He also mentioned the effect of the suction plenum chamber in his statement expressing the agreement between numerical and experimental results. The impact of the BLS strongly depends on the realization of the suction process in the experimental setup especially under low suction flow ratios.

The purpose of the present investigation is to figure out the optimal BLS characters after taking the cavity within the aspirated blade into account and furthermore, to enlighten details about the effects of internal and external environment factors on the suction parameters that would give a guideline for the application of the BLS technology into highly loaded compressors.

2. Suction schemes

The blade profile of the studied rectangular cascades, as illustrated in Fig. 1, was designed in a previous research program aiming at large diffusion factors.
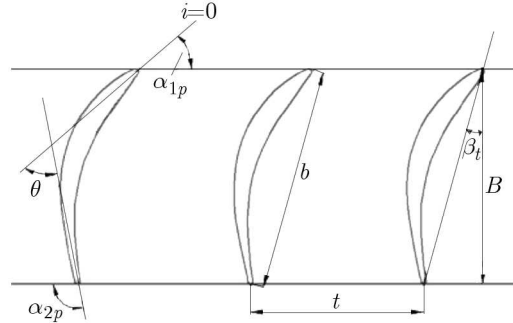

Fig. 1. The cascade and a selected blade profile

The diffusion factor is considered as a reliable indicator of the blade loading capacity; its definition is given as

$$DF = \left(1 - \frac{V_2}{V_1}\right) + \frac{\Delta V_t}{2\sigma V_1} \tag{2.1}$$

The DF of the studied rectangular compressor cascade is computed to be about 0.61, while it turns out to be 0.58 in the wind tunnel experiment. The geometrical parameters of the blade with a suction slot and the aerodynamic parameters of design operating condition are specified in Table 1.

Table 1. Geometrical and aerodynamic parameters

b [mm]	120	β_t [°]	15.3
σ	1.28	w [mm]	2
h [mm]	160	i [°]	0
α_{1p} [°]	40	Re	$5.07 \cdot 10^5$
α_{2p} [°]	100	Ma	0.23

3. Numerical methodology

Simulations of the steady three dimensional viscous flow field were carried out on a highly loaded compressor cascade, using the CFD package ANSYS CFX. Among the existing turbulence models, SST was selected as the working one after comparing several simulation results. The geometric model was meshed using ICEM. One of the meshed aspirated configurations studied in the present paper is shown in Fig. 2. Inlet and outlet boundaries were situated at a distance of 1.25 and 1.75 times of chord length upstream and downstream of the blade, respectively. The numbers of nodes in the radial, circumferential and streamwise directions of the blade passage were 61, 51 and 150, respectively. A butterfly grid topology consisted of an inner H-type core portion encapsulated by an O-type grid domain was used. There were 21 layers of nodes in the O-type grid domain, and y^+ around the blade was kept below a value of 2. The radial and circumferential grid resolutions around the blade surface were increased. In addition, comparisons between the existing and the refined model were carried out to ensure that the predicted results remained closely similar. The total number of nodes in the refined model of the suction schemes was about $7.5 \cdot 10^5$ in the suction schemes. The total pressure of the inlet

boundary was given in form of a profile data which was gained through experiments, while the static pressure at the outlet boundary was kept constant in value. It is noteworthy that in addition to the passage and the suction slot, the simulated region of suction schemes also contained the off-take cavity inside the blade which was one segment of the bleeding channel sharing an interface with the suction slot region. The lower and upper boundaries of the cavity were defined as the outlet with a certain amount of mass flow rate and wall respectively, which was identical to the suction realization of the corresponding experiments (Guo *et al.*, 2010).
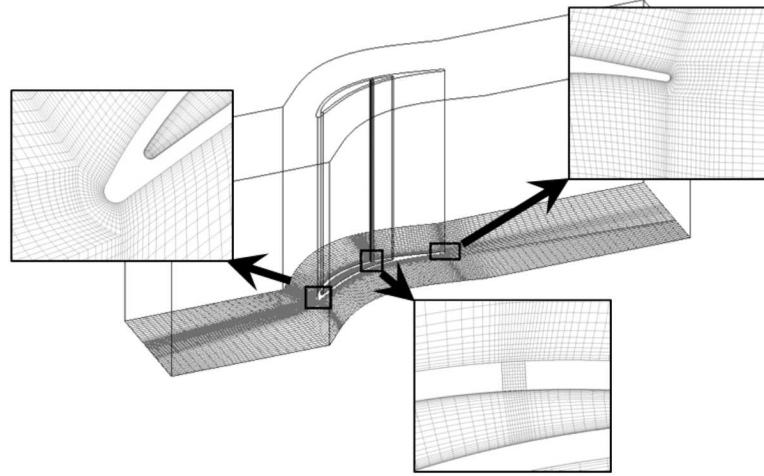

Fig. 2. Mesh for SS4 scheme computation

This suction style is denoted by "one-side-suction" for short in the following paragraphs. And it will be confirmed by this work that the passage flow would be symmetrical about the midspan in principle under one-side-suction manner if the suction device is properly designed. As a result, the suction system could be simplified and deemed effective.

The baseline compressor cascade without the boundary layer suction was denoted by "ORI". Though preliminary experimental investigation was conducted (Guo *et al.*, 2010), ORI and four suction configurations marked by "SS1", "SS2", "SS3" and "SS4" were numerically simulated in this paper to gain more detailed clues which were inconvenient to be obtained in experiments. Besides that, another suction configuration named "SS5" was designed to identify the optimal position and its mechanism. Each suction configuration had a full-span slot perpendicular to the endwalls.
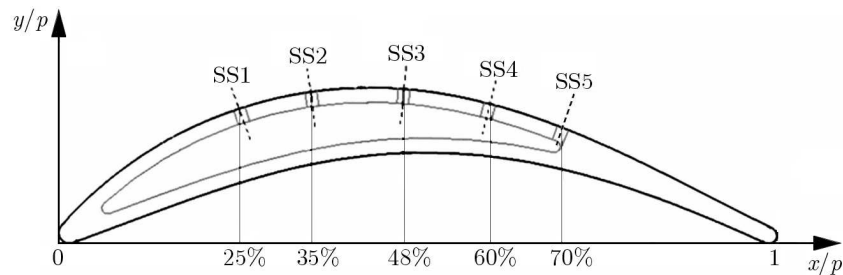

Fig. 3. Location of suction slots in calculation schemes

The slots are $2\,\mathrm{mm}$ wide, equivalent to about 1.7% of the blade chord length. Five suction locations are depicted in Fig. 3. All the suction slots are drilled along the local normal direction of the blade profile. The suction slot of SS5 connects with the blade cavity at the very rear of the cavity. Three different suction flow rates were studied in the present paper which were 0.5%, 1.0% and 1.5% of the inlet flow of the ORI scheme, respectively. They are denoted by $\beta = 0.5\%$, $\beta = 1.0\%$ and $\beta = 1.5\%$ as follows.

A total pressure coefficient is employed to evaluate flow losses in the blade passage. It is defined based on the inlet main flow pressures as shown in Eq. (3.1)

$$\omega = \frac{P_{t0} - P_t}{P_{v0}} \tag{3.1}$$

The pressures of the inlet section are measured by an anemometer fixed at the centre region of the inlet flow. The other pressure is taken by an L-shaped five-hole probe. P_{v0} stands for the kinetic pressure of the inlet flow.

4. Validation of numerical simulation

The applied numerical method was validated against the experimental data. The traverse at 40% of the chord length downstream of the blade trailing edge is considered to be the outlet of the studied cascade. SS4 suction configuration with 1.5% suction flow rate is the most effective in improving the flow field and decreasing cascade losses with the extent of this investigation. Hence, it is selected to depict the comparison between numerical and experimental results in the following paragraphs.
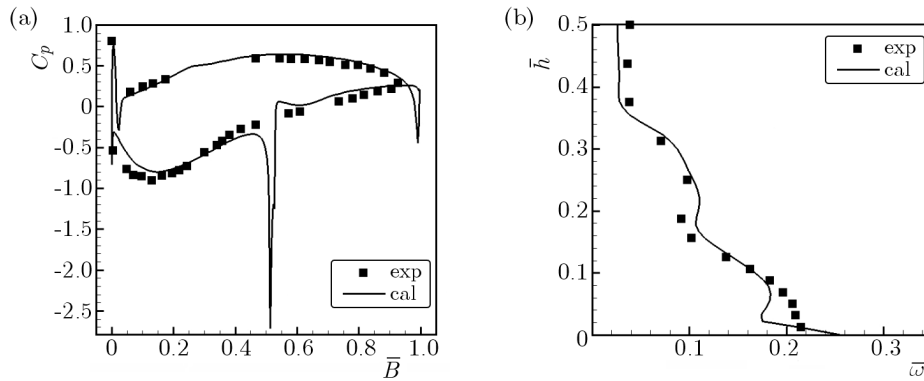

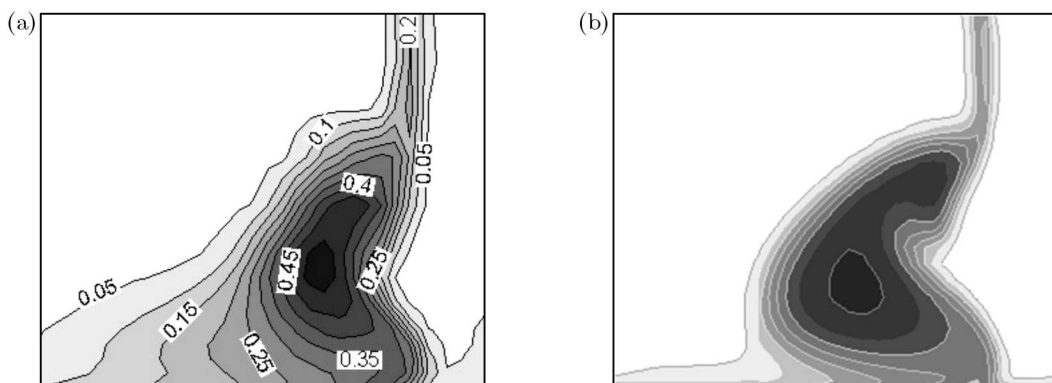Fig. 4. (a) Static pressure coefficient; (b) total pressure loss

Fig. 5. Outlet total pressure loss; (a) experimental result, (b) calculation result

Figures 4a and 4b illustrate the static pressure of the blade surface at 5% blade height and the pitchwise-averaged total pressure loss within the lower half span, respectively. The calculated results are represented by solid lines while the experimental data is symbolized. Figure 5 shows the total pressure loss contours on the cascade outlet. The streak lines on the suction surface and the endwall are displayed in Fig. 6 for comparison. Three dimensional separation lines and

attachment lines in the corner region are quite similar in form. However, the calculation result displays the separating regions more distinctly than the ink-trace visualization.
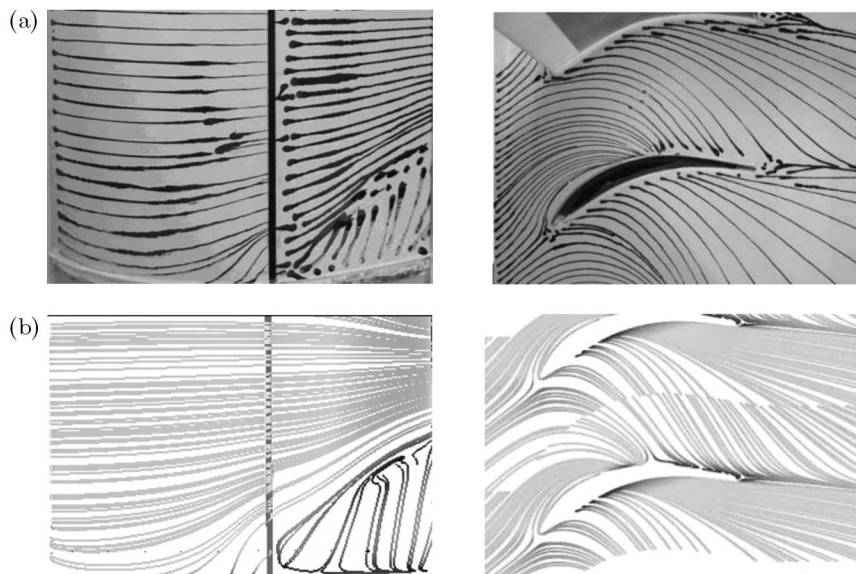

Fig. 6. Ink-trace flow visualization and limiting streamlines; (a) experimental result, (b) calculation result

The contrast between the experimental and numerical results is conspicuous in the loss distribution, particularly around the endwall region. The total loss of the cascade outlet is computed to be about 8.7% in the numerical simulation, 0.7% lower than the experimental data. This difference mainly accounted for two factors. The first is attributed to the measurement error and the disturbance of the experimental facility affecting the nearby flow field. The disturbance gets more obvious when the L-shape five-hole probe locates at those measurement stations which are too close to the endwall. The tiny intervals between the five holes on the probe tip could be ignored when the probe is located in the main flow, and the measured pressure values from all the holes of the probe are assumed to be picked from the very same point. However, this assumption is sort of inaccurate in boundary layer regions with a high velocity gradient. In addition, the in-between fluid may be impelled to accelerate when the head of the probe is equal to or even bigger in size in comparison with the clearance between the probe and the endwall. The second is a consequence of the default setting of the SST turbulent model with the consideration that the solid surfaces are absolutely smooth. In fact, the surface roughness of the steel object after general machining is about $4.6 \cdot 10^{-5}$ m. Nevertheless, most experimental and numerical results are consistent with each other. Thus the validity of the numerical results has been confirmed, and the deduced conclusion owns a high degree of reliability.

5. Results and discussion

The aerodynamic performance of five suction configurations with different suction positions were numerically investigated under several suction flow rates to find the optimal suction position and suction flow rate. There are always primary issues in the BLS application. Figure 7 shows the variation of the overall total pressure loss at the cascade outlet as the suction position varies along the chordwise direction. A higher suction flow rate usually causes an inversely proportional loss reduction. However, the pace gradually slows down in the loss reduction for all these suction configurations when β increases from 0.5% to 1.5%. It becomes more obvious in the suction schemes whose suction location is close to the blade leading edge, such as SS1 and SS2. So it

could be inferred that the performance of the compressor cascade could not be further improved once β exceeds a certain amount, and this limited suction flow rate greatly depends on the thickness and velocity profile of the local boundary layer at the location of suction position. It is also depicted in Fig. 7 that 1.5% is almost the limited suction flow rate for SS1 and SS2, but it is not big enough for SS4. Besides that, the curve of 1.5% suction flow rate fluctuates with a bigger amplitude than the other two, which suggests that the schemes with larger suction flow rate requires more careful consideration on choosing a proper suction location. The optimum suction positions with the minimal overall loss are close to 60% chord under the studied three suction flow rates. SS4 with 1.5% suction flow rate is the most effective in subsiding the cascade loss, and it also coincides with the experimental conclusion (Guo *et al.*, 2010).
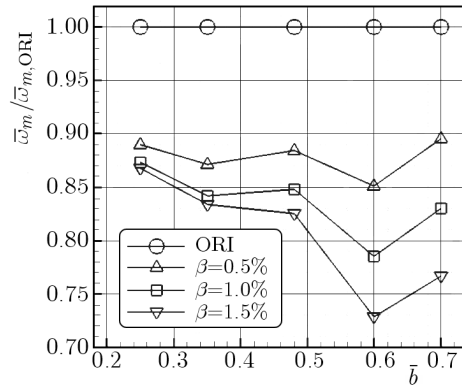

Fig. 7. Variation of overall cascade loss at different suction positions

The SS3, which prevents these curves from spline fitting, seems to be the most discordant configuration among all these suction schemes. It was found that SS3 slot locates just in the region of a two-dimensional separating bubble on the suction surface in the previous wind tunnel experiments, and the aerodynamic improvement of SS3 schemes was not so satisfying.

The reason for SS5 could not surpass SS4 is explored in the following paragraphs. Figure 8 shows limiting streamlines on the suction surface and the outlet loss contour of SS5 when β is 1.5%. Both figures present remarkable asymmetrical structures along the spanwise direction.
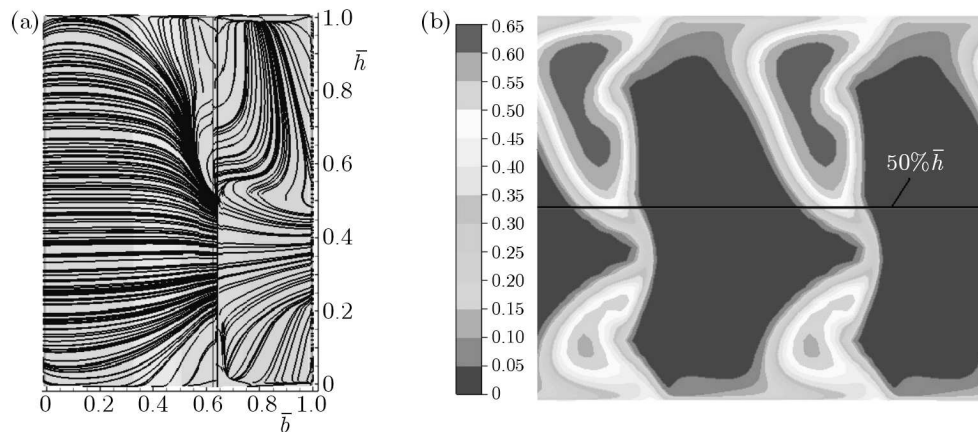

Fig. 8. Calculation results of SS5 scheme at $\beta = 1.5\%$; (a) limiting streamlines on S.S., (b) contour of total pressure loss at cascade outlet

The corner separation as well as the high loss region of the upper half span transfers towards the lower endwall in larger scales and more severe degree compared with that of the ORI case. Obviously, the application of one-side-suction manner should be responsible for the asymmetry phenomena which make SS5 schemes quite unique among all the suction configurations and weaken the advantage of boundary layer suction.

The results with regards to the suction flow rate distribution presented in this paper are all obtained through numerical simulation as it is too hard to be captured in wind tunnel experiments without disturbing the nearby flow field. Figure 9 shows the regulation of the suction flow distribution at the suction slot inlet. The relative blade height $\overline{h}$ is plotted above the area-averaged suction flow rate $\overline{m}$. Most of these curves are basically symmetrical about the midspan as the averaged suction flow rate is low around the midspan and high at both the blade ends. Those curves corresponding to SS1 and SS2 schemes possess a better symmetrical characteristic, and the value of $\overline{m}$ barely changes within a broad range around the midspan. The symmetrical characteristic begins to decline in SS3 schemes, though it still exists. The local suction flow rate around the blade tip is less than that of the blade hub. But this difference only manifests itself in contrast between the two sides of the blade, approximately within 5% blade height. The distinction between the blade hub and tip is increasingly sharp in SS4 schemes, but these curves are still well symmetrical from 20% to $80\%\overline{h}$ with a minimal $\overline{m}$ at the midpan. When the suction slot is connected with the blade cavity at the very ear of the cavity, i.e. in SS5 schemes (refer to Fig. 3), the distribution of $\overline{m}$ completely loses the symmetrical characteristic. The value of $\overline{m}$ gradually reduces from the blade hub to $80\%\overline{h}$ or so, and the variation is especially rapid between the hub and $10\%\overline{h}$. The minimum value of $\overline{m}$ emerges in the upper half span; the local $\overline{m}$ around the endwall is still the highest among the upper half span but just with a slender advantage.

The differences between the five suction configurations in Fig. 9 imply that the spanwise distribution of the suction flow rate lies on both the external and internal influences originated from the adjacent regions of the suction slot. These influences are classified by the spatial relationship between the aspirated blades and adjacent regions.

The external influence is referred as to come from the pressure, the velocity direction and other aerodynamic parameters of the vicinal fluid outside of the aspirated blade, i.e. in the blade passage. The $\overline{m}$ distribution trend, low in the midspan and high at each side of the blade, is mainly resulted from the external influence. As the suction surface boundary layer around the midspan is high in speed but low in pressure, its streamwise velocity is much bigger than that in the spanwise direction. Hence, the corresponding fluid flows out of the region of BLS action in no time. On the contrary, the suction surface boundary layer near the endwall of the cascade just behaves in the opposite way. The low energy fluid is low in speed and high in pressure, and a conspicuous 3D characteristic could be observed as it also flows along the spanwise direction (refer to Fig. 6). This characteristic retards the corresponding low energy fluid from flowing out of the sphere of BLS action. Thus the effect of BLS accumulates. So the fluid is easier to be sucked out from the passage than that around the midspan. The external influence varies with the changes in suction location along the chordwise direction as it is closely linked to the pressure and velocity field around the suction surface. The uneven character of the suction flow distribution along the span becomes more remarkable as the suction location is placed more downstream, i.e. higher at the midspan and lower around the endwalls. The external influence is symmetrical about the midspan because the studied cascade is rectangular in shape, constructed from straight blades. So the spanwise distribution of the suction flow would also be symmetrical about the midspan when the external influence plays the major role, even though the suction facility is asymmetrical.

Moreover, there is another aspect of the external influence in SS4 schemes. Figure 10 compares the results of different suction configurations under each overall suction flow rate. SS4 schemes stand out from all the suction configurations as there are two maximums of the local suction flow rate around $10\%\overline{h}$ and $80\%\overline{h}$ under all these three overall suction flow rates. These two spanwise positions happen to be the same with that of the corner separation lines on the suction surface according to the ink-track visualization in Fig. 6. Therefore, a more low energy fluid which is about to separate from the suction surface could be transferred out from the cascade in
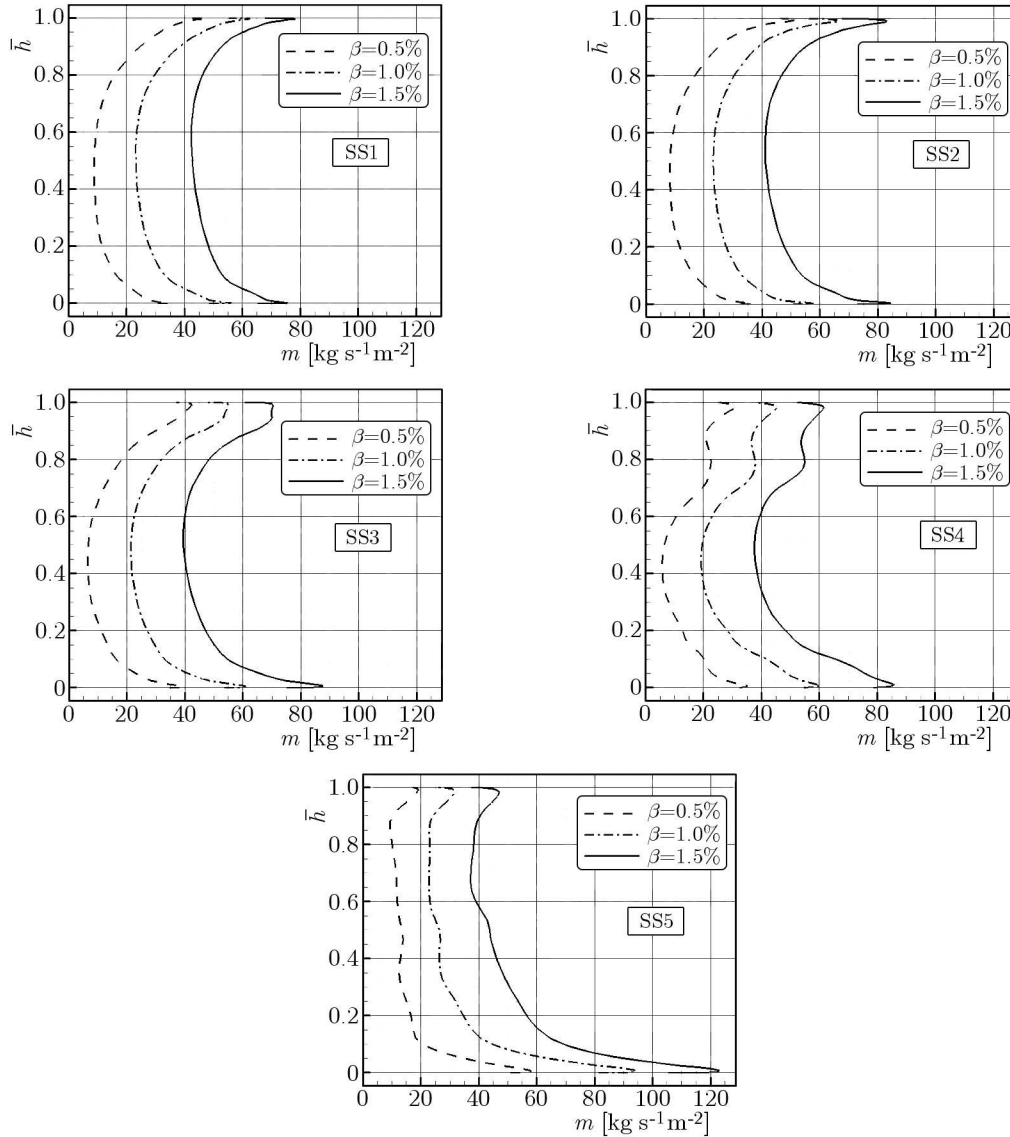
Fig. 9. Spanwise distribution of the suction flow rate under different configurations

SS4 schemes. Here, it is a special advantage of SS4, which also makes an effort in its superiority over the other schemes.

The internal influence, in this paper, refers to that originated from the inner cavity of the aspirated blade. It mainly relates with the local shape of the blade cavity around the suction slot and the one-side-suction manner. The external influence assumes a primary role as the local space of the cavity around the suction slot is spacious enough to let the low energy fluid pass smoothly, such as SS1 and SS2 schemes (see Figs. 3 and 9). In this case, removing the low energy fluid through both the upper and lower endwalls or only through the lower endwall would just results in a similar suction flow distribution. The suction flow would be distributed symmetrically about the midspan as the flow field of the rectangular cascade. But if the inner space is extremely narrow around the suction slot, such as in SS5 schemes (refer to Fig. 3), the transferred fluid will suffer from higher frictional drag along the suction channels, which excites jam to a certain extent. As a result, the inner influence holds the dominant role in affecting the distribution of the suction flow rate and the flow field of the blade passage. As a consequence, the symmetric character which resulted from the external influence is weakened, and the local suction flow rate of the lower half span is much higher than that of the upper half span due
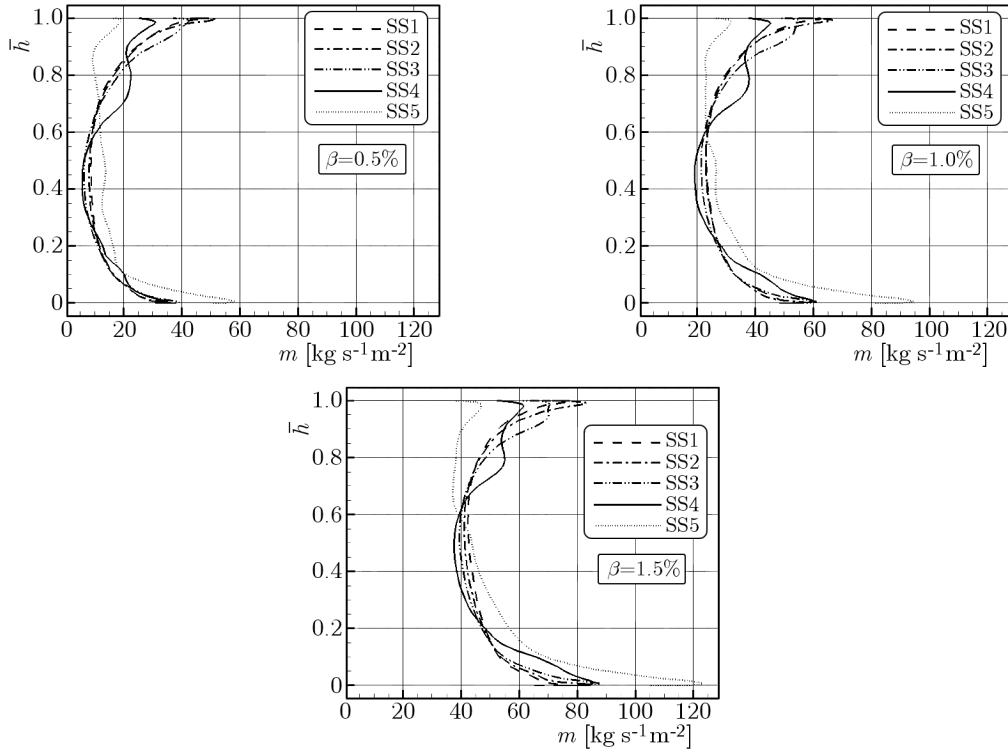
Fig. 10. Spanwise distribution of the suction flow rate at the suction slot inlet

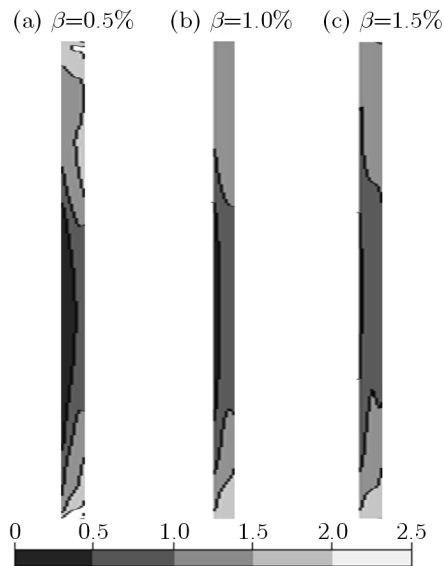(a) β=0.5%   (b) β=1.0%   (c) β=1.5%

Fig. 11. Distribution of the mass flow on the inlet of SS4 slot

to the one-side-suction manner. In addition to this, the area-averaged suction mass flow varies quite rapidly within the lower span. This implies that transferring the low energy fluid through both sides of the aspirated cascade can not reform the highly uneven distribution along the span, if the inner room adjacent to the suction slot is too limited. As the transferred flow would be mainly consisted of the low energy fluid around the ends of the aspirated blade, it is much closer to the outlet of the suction channel.

The amount of the overall suction flow rate is another important factor influencing the distribution of the suction flow. Taking SS4 schemes as an example, Fig. 11 presents the contour of the ratio of the local suction flow rate to the overall averaged suction flow rate on the inlet

section of the suction slot. The aspect ratio of this section is 80; however, it has been scaled to one-fourth of its actual value in Fig. 11 for the sake of visibility. The left and top edges of each rectangular picture stand for the upstream and shroud boundaries of the suction slot inlet, respectively. The difference among the three contours indicates that the distribution of the suction flow rate at the inlet of the suction slot tends to be even and symmetrical as the overall suction flow rate β increases. However, this rule works only when the external influence dominates the suction flow distribution (refer to Fig. 9). Once the internal influence takes charge, the variation of distribution would behave the opposite.

6. Conclusion

Numerical simulations were carried out on highly loaded aspirated compressor cascades to explore the effects of the off-take cavity configuration. The main conclusions of the present paper could be summarized as follows.

1. The regulation of suction flow distribution along the spanwise direction is dictated by both the external and internal influences.

   The aerodynamic parameters of the compressor cascade, namely the external influence, will dominate the distribution when the off-take cavity space around the suction slot is spacious enough to allow the suction flow transfer. The suction flow distribution along the spanwise direction resembles C-type and is symmetrical about the midspan, high at each end and low at the midspan of the blade. The contrast between the maximum and minimum local suction flow rates would be enhanced either by positioning the suction location more downstream or by decreasing the overall suction flow rate. In addition, there will be another local maximum suction flow rate at the intersection between the suction slot and the corner separation line on the suction surface. This will occur if the low energy fluid is about to separate at this junction point; this is more obvious under a high overall suction flow rate.

   The internal influence would take place when the available blade cavity space around the suction slot is too narrow to transfer the suction flow. The applied one-side-suction manner leads to a higher local suction flow rate around the suction side compared to the other side. The asymmetrical distribution of the suction flow also ruins the symmetrical characteristics of the rectangular cascade flow field.

2. The optimal suction location materializes the balance between the external and internal influence. Under all these three studied overall suction flow rates, the optimal suction location is around 60% of the chord downstream the corner separation point and the two-dimensional separation bubble on the suction surface.

3. The one-side-suction manner succeeds in achieving symmetrical distribution under most suction configurations in this paper. Hence, the feasibility of simplifying the suction system is verified, and more attention should be paid to the suction system design while investigating the BLS technology.

References

1. CHEN F., SONG Y., CHEN H., WANG Z., 2006, Effects of boundary layer suction on the performance of compressor cascades, *ASME Paper*, **GT2006-90082**

2. CHEN F., SONG Y., ZHAO G., LIU J., WANG Z., 2005, Effects of boundary layer suction on the performance of compressor cascade with different solidities, *Journal of Engineering Thermophysics*, **26**, 2, 211-215

3. GMELIN CH., THIELE F., LIESNER K., MEYER R., 2011, Investigations of secondary flow suction in a high speed compressor cascade, *ASME Paper*, **GT2011-46479**

4. GUO S., CHEN S., SONG Y., SONG Y., CHEN F., 2010, Effects of boundary layer suction on aerodynamic performance in a high-load compressor cascade, *Chinese Journal of Aeronautics*, *23*, 2, 179-186

5. KERREBROCK J.L., DRELA M.A., MERCHANT A., SCHULER B.J., 1998, A family of designs for aspirated compressors, *ASME Paper*, **98-GT-196**

6. KERREBROCK J.L., REIJNAN D.P., ZIMINSKY W.S., SMILG L.M., 1997, Aspirated compressors, *ASME Paper*, **97-GT-525**, Orlando

7. LOUGHERY R., HORN R.A., 1971, Single stage experimental evaluation of boundary layer blowing and bleed techniques for high lift stator blades, *NASA, CR-54573*

8. MERCHANT A.A., DRELA M., KERREBROCK J.L., ADAMCZYK J.J., CELESTINA M., 2000, Aerodynamic design and analysis of a high pressure ratio aspirated compressor stage, *ASME Paper*, **2000-GT-619**

9. MERCHANT A.A., KERREBROCK J.L., ADAMCZYK J.J., BRAUNSCHEIDEL E., 2004, Experimental investigation of a high pressure ratio aspirated fan stage, *ASME Paper*, **GT2004-53679**

10. REIJNEN D.P., 1997, Experimental study of boundary layer suction in a transonic compressor, PhD Thesis, Cambridge, MA: MIT, January

11. SCHULER B.J., KERREBROCK J.L., MERCHANT A.A., DRELA M., ADAMCZYK J., 2000, Design, analysis, fabrication and test of an aspirated fan stage, *ASME Paper*, **2000-GT-618**

12. SONG Y., CHEN F., JANG J., WANG Z., 2005, A numerical investigation of boundary layer suction in compound lean compressor cascades, *ASME Paper*, **GT2005-68441**

13. WANG Y., GUO R., ZHAO L., REN S., 2012, Numerical investigation on the effects of re-organized shock waves on the flow separation for a highly-loaded transonic compressor cascade, *Journal of Thermal Science*, **21**, 1, 13-20

14. WENNERSTROM A.J., 1990, Highly loaded axial flow compressor history and current development, *Journal of Turbomachinery*, **112**, 567-578

15. ZHAO S., LUO J., LU X., ZHU J., 2010, Exploring the intention of using aspirated cascade to replace tandem cascades, *Journal of Thermal Science*, **19**, 5, 390-396